Force Sensorless Control of Cutting Resistance for NC Machine Tools by Spindle Motor Control Using Variable Pulse Number T-method

Teruaki Ishibashi and Hiroshi Fujimoto
Department of Advanced Energy, The University of Tokyo
5-1-5, Kashiwanoha, Kashiwa, Chiba, 227-8561 Japan
Phone: +81-4-7136-3881, Fax: +81-4-7136-3881
Email: ishibashi@hflab.k.u-tokyo.ac.jp, fujimoto@k.u-tokyo.ac.jp

***Abstract*— This paper proposes a force sensorless control of cutting resistance for numerical control (NC) machine tools by spindle motor. In conventional NC machine tools, speed of spindle motor is set to a constant value during machining, and the spindle speed is determined according to operator's experience. The proposed method estimates cutting resistance by disturbance observer, and the spindle speed is determined by controlling the cutting resistance to follow the reference value. In addition, a novel method for velocity calculation which is referred as variable pulse number T-method is proposed to reduce the velocity measurement noise and to improve the robustness of disturbance observer.**

I. Introduction

Recently, NC machine tools play an important role as mother machine in industry. A considerable amount of study has been done on the NC machine tools to realize high accuracy and high speed of machining [1][2]. Cutting resistance, chatter vibration and thermal expansion have negative effect on cutting accuracy. Chatter vibration is the vibration of tool excited by certain factor [3][4].

Cutting resistance is observed carefully because it causes many problems during machining, such as chatter vibration, deflection of tool and so on. Usually, force sensor or acceleration sensor are implemented to observe cutting resistance, which is not practical due to the cost and difficulty. Some previous studies have proposed methods to predict and control the cutting resistance [5][6]. However, the methods are not practical, because they need test cutting and identifying many parameters of tool which are difficult to measure.

In this study. a model of cutting resistance is proposed, and control of the cutting resistance by spindle speed control is proposed based on the model. This method does not need additional sensor because cutting resistance is estimated by disturbance observer [7][8]. Moreover, the proposed approach is not affected by the decreasing of inertia of stage during machining. In addition, a novel method to measure angular velocity is proposed to suppress noise effects in disturbance observer.

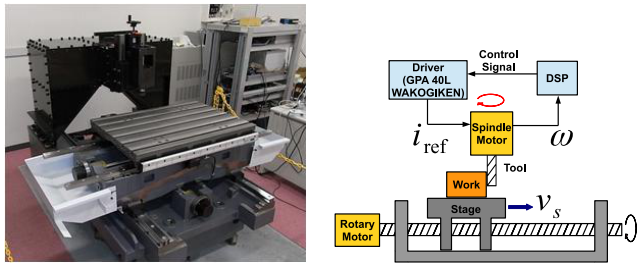

(a) Equipment overview. (b) Schematic diagram of plant.

Fig. 1. Experimental equipment.

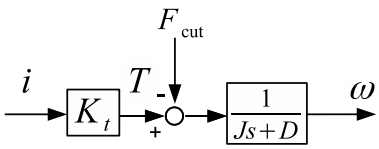

Fig. 2. Block diagram of plant.

II. Controlled System

This section will introduce the experimental plant and simplified cutting resistance model.

A. Spindle motor

Fig. 1(a) shows an overview of experimental equipment, and Fig. 1(b) shows a schematic diagram of plant during machining. Machining is performed by feeding stage and pressing a work against tools. Cutting resistance arise during machining. In this paper, cutting resistance is controlled by spindle speed. The feed rate is set to a constant value during machining. Fig. 2 shows block diagram of plant. Here, v_s is the feed rate, i is current, K_t is torque coefficient, and T is torque. The torque is acquired by (1).

$$T = K_t i. \tag{1}$$

Cutting resistance is considered as a disturbance torque to spindle and denoted as F_{cut}. Other disturbance factors are not taken into account because the volumes are quite smaller than

TABLE I

PARAMETERS OF SPINDLE

Driver	GPA40L
Inertia J	4.4×10^{-3} kg $\cdot$ m^2
Friction coefficient D	2×10^{-3} Nm $\cdot$ s
Torque coefficient K_t	0.92 Nm/A

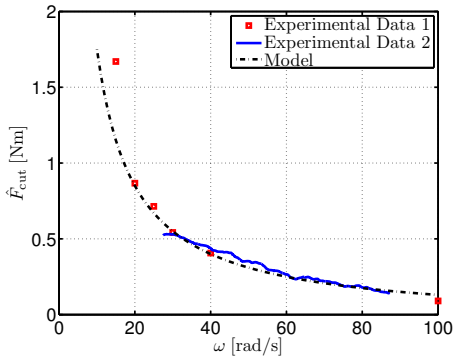

(a) Relationship between cutting resistance and angular velocity

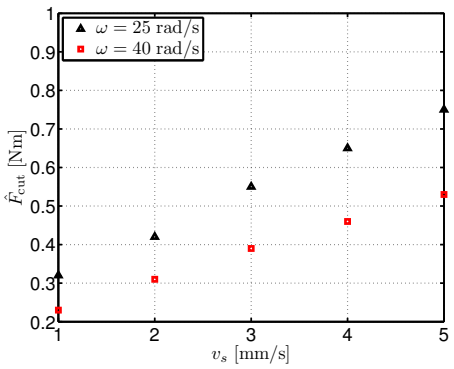

(b) Relationship between cutting resistance and feed rate

Fig. 3. Measurements of cutting resistance.

cutting resistance. Spindle speed is acquired by (2). Here, J is inertia of spindle including tools, D is friction coefficient of spindle, ω is spindle speed. Table 1 shows parameters of spindle and driver.

$$\omega = \frac{1}{Js + D}(T - F_{\rm cut}). \tag{2}$$

B. Cutting resistance model

Simplified cutting resistance model is acquired by (3). This model assumes that cutting resistance is proportional to thickness of swarf. Here, k is a coefficient depending on axial depth, radial depth, temperature, quality of work and so on. We denote this parameter as cutting resistance coefficient in the following.

$$F_{\rm cut} = k\frac{v_s}{\omega}. \tag{3}$$

Fig. 3(a) shows the relation between spindle speed ω and cutting resistance $\hat{F}_{\rm cut}$ estimated by disturbance observer. In experiment, a chemical wood is used as work, and v_s, axial depth and radial depth is set as 4 mm/s, 5 mm and 14 mm, respectively. Experimental data 1 is measured at $\omega = 15, 20, 25, 30, 40, 100$ rad/s and Experimental data 2 is at $\omega = 27 \sim 88$ rad/s. In experimental data 2, the measurement was performed with a ramp speed signal. Fig. 3(b) shows the relation between feed rate v_s and cutting resistance $\hat{F}_{\rm cut}$ estimated by disturbance observer.

These data show that cutting resistance has inverse relation with spindle speed and proportional relation with feed rate. Control system is designed according to the simplified cutting resistance model.

III. ANGULAR VELOCITY MEASUREMENT METHOD

This section presents conventional method and a novel method to measure angular velocity.

A. Conventional velocity estimation methods

In order to measure Angular velocity, M-method, T-method [9], S-method [10], M-method-based method using FPGA [11], and Average T-method [12] are commonly used. In the M-method, the angular velocity is calculated by counting the number of encoder pulses within one sampling. In contract, T-method calculates angular velocity by measuring the period of one encoder pulse using base-clock of DSP. Accuracy of M-method and T-method is degraded in the low-speed area and high-speed area, respectively. S-method calculates the velocity synchronized with the variation of number of the encoder pulse counted in a sampling time. S-method can measure angular velocity with higher accuracy in all-speed areas. In average T-method, angular velocity is calculated by measuring the period of N_p encoder pulses using base-clock of DSP. It can measure angular velocity with high accuracy in more higher-speed area than T-method. N_p is set as constant during measuring in average T-method, . So, it cannot be applied to the situation that angular velocity varies due to the phase-lag and reduce the accuracy.

Variable pulse number T-method is novel method based on average T-method taking the variation of velocity into consider. In this method, N_p changes during measuring according to angular velocity. The algorithm is described in subsection C.

B. Detection accuracy

Fig. 4 shows the principle of angular velocity measurement. Here, P is resolution of encoder, T_s is sampling period. N_s is number of the pulse counted within one sampling period, $T_{\rm clock}$ is resolution of base-clock, $T_{1p}[i]$ is the actual period of a encoder pulse, $\hat{T}_{1p}[i]$ is measured $T_{1p}[i]$ by base-clock, $T_{Np}[i]$ is the actual period of N_p encoder pulses, and $\hat{T}_{Np}[i]$ is measured $T_{Np}[i]$ by base-clock.

Computing equations of each method are (4)$\sim$(6). ω_m, ω_t and ω_a are angular velocity measured by M-method, T-method

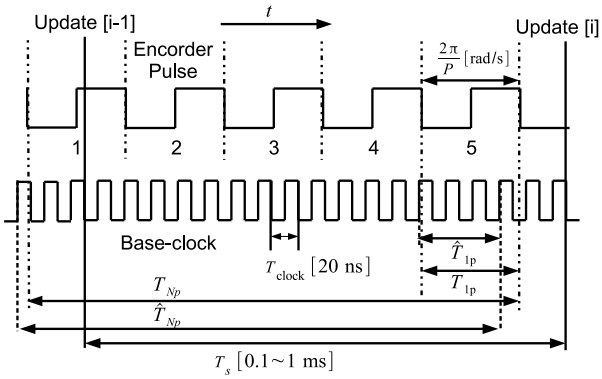

Fig. 4. Principle of angular velocity detection.

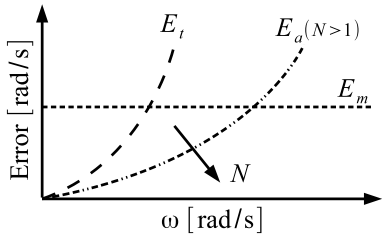

Fig. 5. Angular velocity detection error.

and average T-method, respectively.

$$\omega_m[i] = \frac{2\pi N_s[i]}{P}\frac{1}{T_s}. \quad (4)$$

$$\omega_t[i] = \frac{2\pi}{P}\frac{1}{\hat{T}_{1p}[i]}. \quad (5)$$

$$\omega_a[i] = \frac{2\pi N_p[i]}{P}\frac{1}{\hat{T}_{Np}[i]}. \quad (6)$$

In M-method, detection error arises due to the resolution of encoder. In contrast, in T-method and average T-method, detection error arises due to the resolution of base-clock. Fig. 5 shows the detection error. Here, E_m, E_t and E_a are maximum detection error using M-method, T-method and average T-method, respectively. Each value is acquired by (7)∼(9). Here, $\hat{T}_{Np}$ is approximated by $N_p\hat{T}_{1p}$. Assuming T_{clock} is much smaller than T_{1p}, the detection error of average T-method is reduced to $1/N_p$ compared with T-method.

$$E_m[i] = \frac{2\pi}{P \cdot T_s}. \quad (7)$$

$$E_t[i] = \frac{2\pi}{P}\frac{T_{\mathrm{clock}}}{\hat{T}_{1p}[i](\hat{T}_{1p}[i] + T_{\mathrm{clock}})}. \quad (8)$$

$$E_a[i] = \frac{2\pi}{P}\frac{T_{\mathrm{clock}}}{\hat{T}_{1p}[i](N_p\hat{T}_{1p}[i] + T_{\mathrm{clock}})}. \quad (9)$$

C. Variable pulse number T-method

The procedure of variable pulse number T-method is shown as follows.

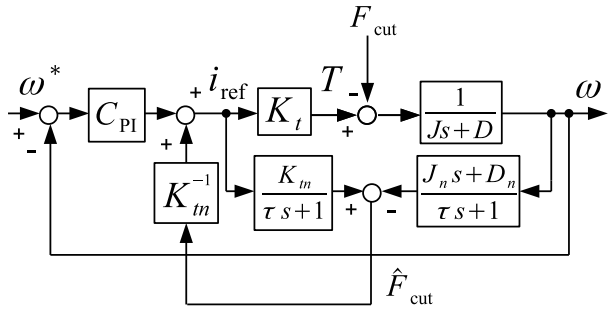

Fig. 6. Block diagram of angular velocity control

1) Count up the pulse number $N_p[i]$ synchronized with encoder signal.
2) Measure the $T_{Np}[i]$ synchronized with counting up $N_p[i]$.
3) Calculate angular velocity by (10) at every sampling period.

$$\omega_v[i] = \frac{2\pi N_p[i]}{P}\frac{1}{\hat{T}_{Np}[i]}. \quad (10)$$

Here, ω_v is angular velocity measured by variable pulse number T-method.

IV. Cutting resistance control system

This section will present the details of cutting resistance control.

A. Speed control system

Fig. 6 shows the block diagram of angular velocity control. C_{PI} is feedback controller which is designed to have a bandwidth of $\omega_p = 100\ \mathrm{rad/s}$ by pole placement method. The parameters of C_{PI} are represented as (11) (12). Disturbance observer is used to estimate and compensate the cutting resistance. Here, τ denotes the time constant of LPF, which is assigned as $1/(2\pi \cdot 200)$ s.

$$C_{\mathrm{PI}} = \frac{K_{\mathrm{P}}s + K_{\mathrm{I}}}{s}. \quad (11)$$

$$K_{\mathrm{P}} = \frac{2J\omega_p - D}{K_{tn}}, \quad K_{\mathrm{I}} = \frac{J\omega_p^2}{K_{tn}}. \quad (12)$$

B. Estimation of cutting resistance coefficient

In proposal method, cutting resistance coefficient is estimated using least-square method. The output y is represented as (13) on the assumption that y is the product of unknown parameter η and known parameter θ.

$$y = \theta\eta. \quad (13)$$

Here, y, η and θ correspond to cutting resistance $\hat{F}_{\mathrm{cut}}$, cutting resistance coefficient k and v_s/ω, respectively. In this way, k can be estimated by least-square method.

Cutting resistance varies according to the angle of the tools. In order to average cutting resistance in the period in which tools rotate n_r times (n_r:integer), the data used to estimation

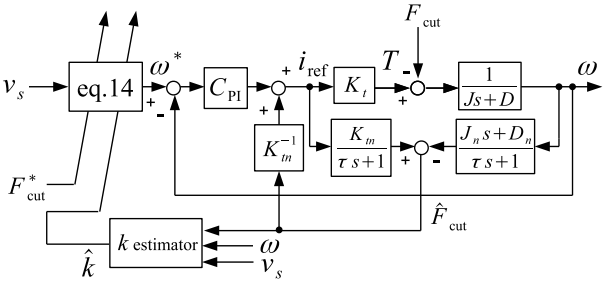

Fig. 7. Block diagram of cutting resistance control.

is limited to those obtained in the period. $\hat{k}$ is updated in every control period.

C. Spindle speed reference

Fig. 7 shows block diagram of cutting resistance control. Spindle speed reference is generated based on cutting resistance model (14).

$$\omega^* = \frac{\hat{k}}{F^*_{\mathrm{cut}}} v_s. \tag{14}$$

V. Simulation results of variable pulse number T-method

This section present simulation results of angular velocity detection.

Resolution of encoder and base-clock are set to $(8000\,\mathrm{Pulse/Rev})$ and $20\,\mathrm{ns}$, respectively. Sampling time of M-method and variable pulse number T-method is set to $1\,\mathrm{ms}$. Taking account of ripple of angular velocity, N_p of average T-method is conservatively set to $N_p = 100$ so that updating cycle would lower than the sampling time.

Fig. 8(a) and Fig. 8(b) show detected angular velocity when motor rotates with a velocity of $104.825\,\mathrm{rad/s}$. Fig. 8(c) shows N_p of variable pulse number T-method. It is obvious that variable pulse number T-method can reduce detection error compared with M-method, T-method and average T-method. It is concluded that variable pulse number T-method can use as much N_p as possible, while average T-method should use conservatively set N_p.

VI. Experiment

This section presents experimental result of angular velocity detection and cutting resistance control.

A. Experimental results of variable pulse number T-method

This section compares M-method, T-method, average T-method, variable pulse number T-method. In the experiment, incremental encoder $(2000\,\mathrm{Pulse/Rev})$ is used and quadrupled in M-method. Resolution of base-clock is $20\,\mathrm{ns}$ and sampling time of M-method and variable pulse number T-method is set to $1\,\mathrm{ms}$. N_p is set conservatively so that updating cycle would lower sampling time $1\,\mathrm{ms}$ in average T-method. Experiment was performed by angular velocity control shown in Fig. 6 with constant angular velocity reference, and angular velocity measured by M-method was used as feedback.

Fig. 9(a) and Fig. 9(c) show experimental results of angular velocity detection. Fig. 9(b) and Fig. 9(d) show N_p of variable pulse number T-method. Reference value of angular velocity was set to $\omega^* = 15, 50\,\mathrm{rad/s}$. In average T-method, N_p was set to $3, 12$. N_p of variable pulse number T-method is as large as possible and it is larger than that of average T-method.

Fig. 10 show estimated cutting resistance measured by disturbance observer using M-method and variable pulse number T-method. When machining, spindle speed was set as constant at $\omega^* = 20\,\mathrm{rad/s}$, and feed rate is set as $v_s = 2, 3\,\mathrm{mm/s}$. By applying variable pulse number T-method, the noise caused by detection error is reduced.

TABLE II
Cutting condition

End mill	KOBELCO 4MC (2 flutes)
End mill ϕ	12 mm
Work piece	Artificial timber MBO600
Free length of end mill	74 mm
Radial depth of cut	6 mm
Axial depth of cut	14 mm

B. Experimental results of cutting resistance control

Experiment was performed under the condition showed in Table. 2. Sample data used to estimating cutting resistance coefficient k is limited to the data obtained in a period in which spindle rotate 1, 2 times ($n_r = 1, 2$). Reference value of cutting resistance is $F^*_{\mathrm{cut}} = 0.3\,\mathrm{Nm}$. Machining starts at $t = 0\,\mathrm{s}$.

Fig. 11 shows the experimental results of conventional method. In conventional method, reference value of spindle speed was obtained by cutting test. There is error between reference value and averaged cutting resistance. This error is caused by inhomogeneous quality of work and some changes in cutting condition.

Fig. 12 and Fig. 13 show experimental results of proposal method. In this method, lower limit was set so that spindle speed does not fall below $15\,\mathrm{rad/s}$. By estimating cutting resistance coefficient k during machining, spindle speed reference ω^* changes and cutting resistance follows the reference value. Convergence speed of estimating reduces with the increasing of n_r. Even when $n_r = 1$, cutting resistance can follow reference value. So, $n_r = 1$ is adequate in this cutting condition.

VII. Conclusion

In this paper, Force sensorless cutting resistance control by spindle motor is proposed. By the experiment, it is confirmed that proposal method can make cutting resistance follow reference value. In order to improve accuracy of disturbance observer, a novel method of angular velocity measurement "variable pulse number T-method" was proposed. By the simulation and the experiment, effectiveness of this proposal method was confirmed.

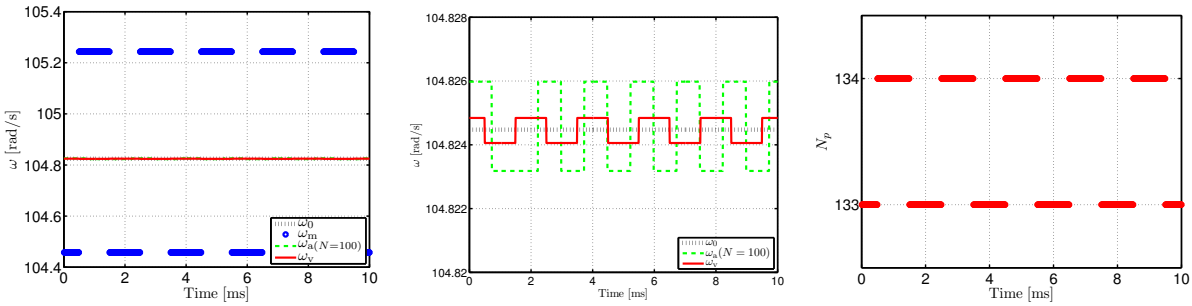

(a) Detected angular velocity

(b) Detected angular velocity (enlarged view)

(c) Counted number of pulse

Fig. 8. Simulation results of angular velocity detection.

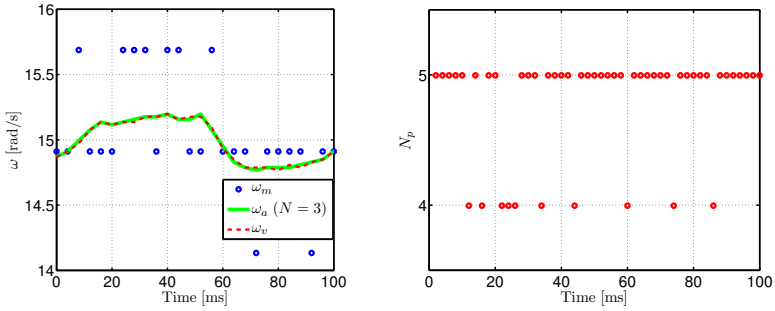

(a) Detected angular velocity ($\omega^* = 15$ rad/s).

(b) Counted number of pulse (VPNT-method) ($\omega^* = 15$ rad/s).

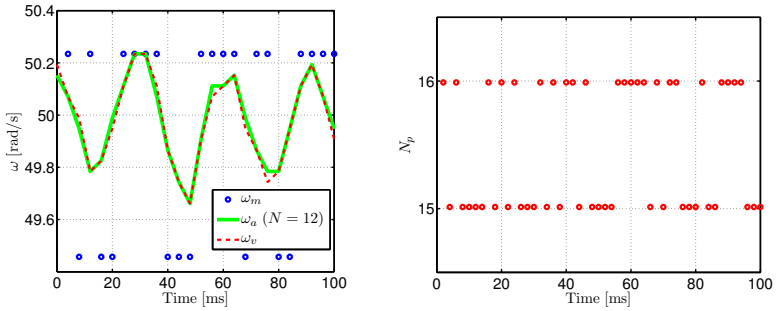

(c) Detected angular velocity ($\omega^* = 50$ rad/s).

(d) Counted number of pulse (VPNT-method) ($\omega^* = 50$ rad/s).

Fig. 9. Experiment results of angular velocity detection.

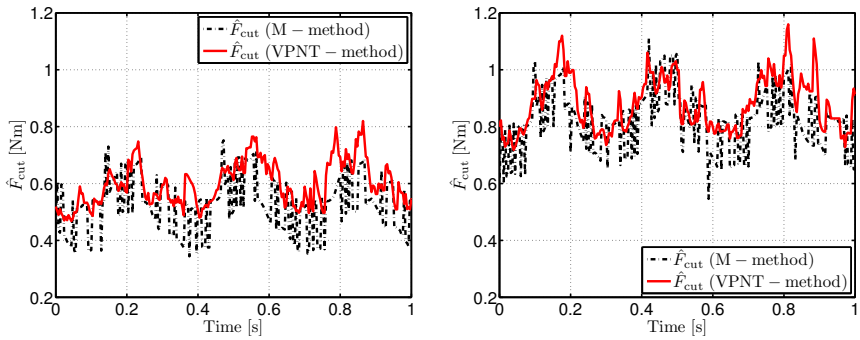

(a) Estimated cutting resistance ($v_s = 2$ mm/s).

(b) Estimated cutting resistance ($v_s = 3$ mm/s).

Fig. 10. Experiment results of estimated cutting resistance by dusturbance observer.

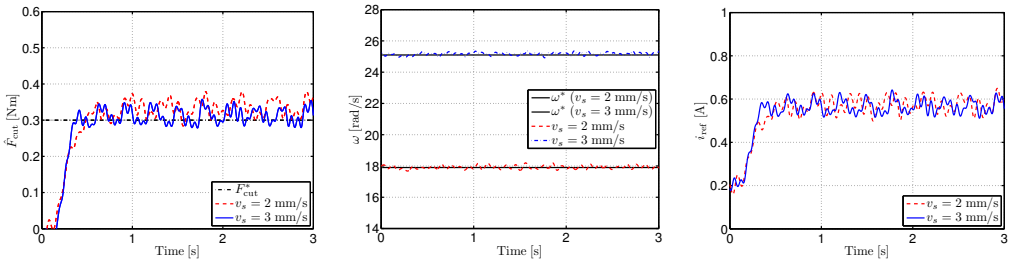

(a) Cutting resistance $\hat{F}_{\rm cut}$. (b) Angular velocity of spindle ω. (c) Current command $i_{\rm ref}$.

Fig. 11. Experimental results (conventional method).

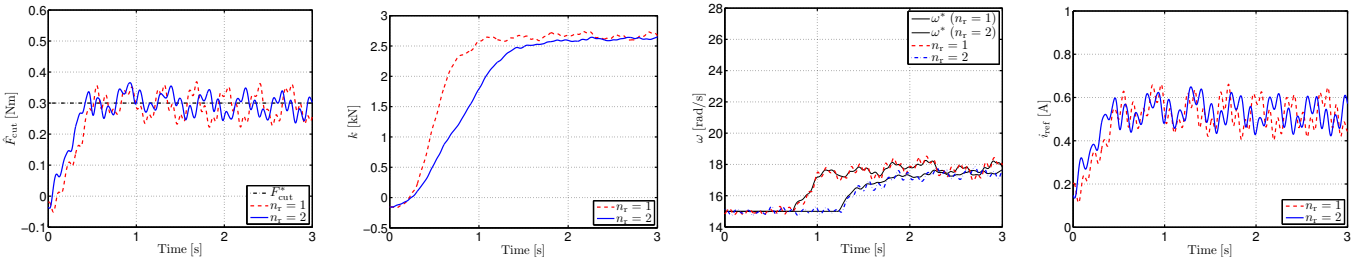

(a) Cutting resistance $\hat{F}_{\rm cut}$. (b) Cutting resistance coefficient k. (c) Angular velocity of spindle ω. (d) Current command $i_{\rm ref}$.

Fig. 12. Experimental results (proposed method $v_s = 2$ mm/s).

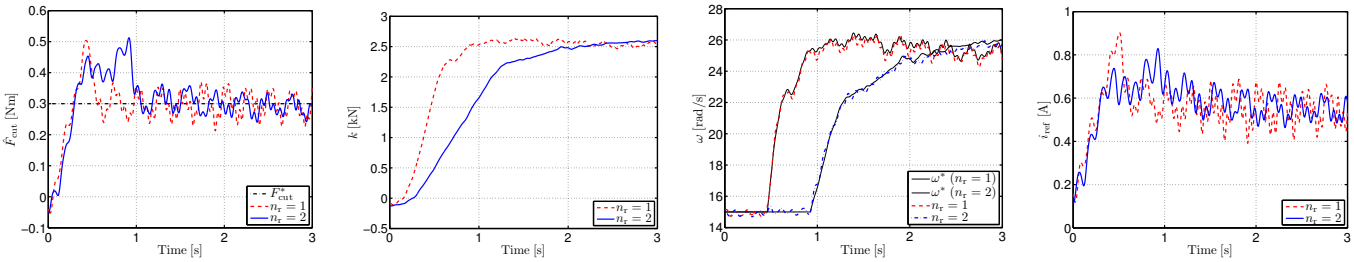

(a) Cutting resistance $\hat{F}_{\rm cut}$. (b) Cutting resistance coefficient k. (c) Angular velocity of spindle ω. (d) Current command $i_{\rm ref}$.

Fig. 13. Experimental results (proposed method $v_s = 3$ mm/s).

VIII. Acknowledgment

This work was supported in part by the MORI SEIKI Co.Ltd.. The authors gratefully acknowledge valuable suggestions from Shinji ISHII, Kouji YAMAMOTO and Yuki TER ADA from the MORI SEIKI Co. Ltd..

References

[1] Z. Jamaludin, H. Van Brussel and J. Swevers, "Quadrant Glitch Compensation using Friction Model–Based Feedforward and an Inverse–Model–Based Disturbance Observer", IEEE Transaction on Industrial Electronics, Vol. 56, No. 10, pp. 3848–3853, 2009.

[2] Y. Maeda and M. Iwasaki, "Improvement of Settling Performance by Initial Value Compensation Considering Rolling Friction Characteristic", The 36th Annual Conference of the IEEE Industrial Electronics Society, pp. 1896–1901, 2010.

[3] S. Seguy, T. Insperger, L. Arnaud, G. Dessein and G. Peigné, "Suppression of period doubling chatter in high–speed milling by spindle speed variation", Machining Science and Technology, Vol. 15, pp. 153–171, 2011.

[4] K. Akazawa and E. Shamoto, "Study on Regenerative chatter vibration in ball end milling of flexible workpieces", Micro–NanoMechatronics and Human Science, pp. 1–6, 2008.

[5] H. Chen, D. Li, S. Huang and P. Fu, "Study on the cutting force prediction of supercritical material millling", ICNC, Vol. 3, pp. 1148–1152, 2010.

[6] K. Mehdi and J.–F. Rigal, "A numerical model for cutting process simulation and prediction of cutting forces in peripheral milling", IEEE ICIT, Vol. 2, pp. 734–740, 2004.

[7] H. Shinno, H. Hashizume and H. Yoshioka, "Sensor-less monitoring of cutting force during ultraprecision machining", CIRP Annals Manufacturing Technology, Vol. 52, Issue. 1, pp. 303–306, 2003.

[8] D. Kurihara, Y. Kakinuma and S. Katsura, "Sensor-less cutting force monitoring using parallel disturbance observer", International Journal of Automation Technology, Vol. 3, No. 4, pp. 415–421, 2009.

[9] T. Ohmae, T. Matsuda, K. Kamiyama and M. Tachikawa, "A Microprocessor-Controlled High-Accuracy Wide-Range Speed Regulator for Motor Drives, IEEE Transactions, Volume. IE-29, Issue. 3, pp. 207–211, 1982.

[10] T. Tsuji, T. Hashimoto, H. Kobayashi, M. Mizuochi and K. Ohnishi, "A wide-range velocity measurement method for motion control", in IEEE Trans. Industrial Electronics, Vol. 56, No. 2, pp. 510–519, 2009

[11] N. Nandayapa, C. Mitsantisuk and K. Ohishi, "High performance velocity estimation for controllers with short processing time by FPGA", IEEJ Journal of Industry applications, Vol. 1, No. 1, pp. 55–61, 2012.

[12] Y. Lakinuma, Y. Sudo and T. Aoyama, "Detection of chatter vibration in end milling applying disturbance observer'", Annals of the CIRP, Vol.60, No. 1, pp. 109–112, 2011.